LETTERS

Endothelial tubes assemble from intracellular vacuoles *in vivo*

Makoto Kamei[1], W. Brian Saunders[3], Kayla J. Bayless[3], Louis Dye[2], George E. Davis[3] & Brant M. Weinstein[1]

The formation of epithelial tubes is crucial for the proper development of many different tissues and organs, and occurs by means of a variety of different mechanisms[1]. Morphogenesis of seamless, properly patterned endothelial tubes is essential for the development of a functional vertebrate circulatory system, but the mechanism of vascular lumenization *in vivo* remains unclear. Evidence dating back more than 100 years has hinted at an important function for endothelial vacuoles in lumen formation[2]. More than 25 years ago, in some of the first endothelial cell culture experiments *in vitro*, Folkman and Haudenschild described "longitudinal vacuoles" that "appeared to be extruded and connected from one cell to the next"[3,4], observations confirmed and extended by later studies *in vitro* showing that intracellular vacuoles arise from integrin-dependent and cdc42/Rac1-dependent pinocytic events downstream of integrin–extracellular-matrix signalling interactions[5–10]. Despite compelling data supporting a model for the assembly of endothelial tubes *in vitro* through the formation and fusion of vacuoles, conclusive evidence *in vivo* has been lacking, primarily because of difficulties associated with imaging the dynamics of subcellular endothelial vacuoles deep within living animals. Here we use high-resolution time-lapse two-photon imaging of transgenic zebrafish to examine how endothelial tubes assemble *in vivo*, comparing our results with time-lapse imaging of human endothelial-cell tube formation in three-dimensional collagen matrices *in vitro*. Our results provide strong support for a model in which the formation and intracellular and intercellular fusion of endothelial vacuoles drives vascular lumen formation.

We were able to visualize vacuolar structures in living human vascular endothelial cells (ECs) cultured *in vitro* in three-dimensional (3D) collagen gel matrices by using light microscopy, the uptake of carboxyrhodamine or the expression of transgenes preferentially localizing to these structures (Fig. 1a–e). Large intracellular vacuoles are clearly visible within human ECs in 3D culture during lumen formation (Fig. 1a) and are readily labelled by uptake of carboxyrhodamine from the medium (Fig. 1b), indicating that they are pinocytic vacuoles. As we have described previously[5,8–10], we could also visualize pinocytic vacuolar structures in living ECs by perivacuolar localization of enhanced green fluorescent protein (EGFP)–cdc42wt (in which 'wt' represents wild-type) fusion protein (Fig. 1c). The cdc42 protein is prenylated with a C_{20} geranylgeranyl group for membrane localization[11], so to provide an independent method of highlighting endothelial vacuoles in living cells we added a farnesylation site membrane localization signal[12] (designated by the suffix '-F') to EGFP or mRFP1 (monomeric red fluorescent protein[13]). When expressed in ECs cultured in 3D collagen gels, EGFP-F protein displays perivacuolar localization (Fig. 1d–f).

To permit observation of the dynamics of endothelial vacuoles and their role in vascular lumen formation *in vivo*, we expressed EGFP–cdc42wt or mRFP1-F in zebrafish ECs. The optical clarity and accessibility of zebrafish embryos and larvae make this an excellent model for imaging the dynamics of blood vessel formation *in vivo*[14,15]. We began by establishing that ubiquitous expression of either EGFP–cdc42wt or mRFP1-F does not cause developmental defects in zebrafish embryos (data not shown). We then prepared constructs to drive the expression of these genes under the control of the zebrafish *fli1* promoter, which we have used previously to drive endothelial expression in transgenic zebrafish[16]. We injected *fli1:EGFP–cdc42wt* DNA into zebrafish embryos and derived a germline transgenic line, *Tg(fli1:EGFP–cdc42wt)^{y48}*, expressing EGFP–cdc42wt in angioblasts and ECs throughout the animal (see Methods). The *Tg(fli1:EGFP–cdc42wt)^{y48}* animals grow and develop indistinguishably from non-transgenic siblings, and adults have normal viability and fecundity (data not shown). We did not observe

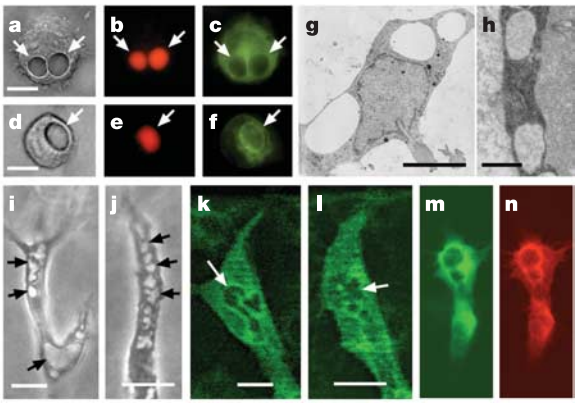

Figure 1 | Imaging of vacuoles in ECs *in vitro* and *in vivo*. **a**–**f**, Vacuoles (arrows) in living human umbilical-vein vascular ECs (HUVEC) cultured in 3D collagen gel matrices, revealed by light microscopy (**a**, **d**), epifluorescence of endocytosed carboxyrhodamine (**b**, **e**), and epifluorescence of either *EGFP–cdc42wt* (**c**) or *EGFP-F* (**f**) transgenes. **g**, **h**, Vacuolar structures revealed in transmission electron micrographs of fixed ECs in 3D EC cell cultures (**g**) or in the developing wall of the zebrafish dorsal aorta 24 h after fertilization (**h**). **i**, **j**, High-resolution light microscopic imaging of vacuoles (arrows) in EC in 3D culture *in vitro*. **k**, **l**, High-resolution multiphoton imaging of growing intersegmental vessels in *Tg(fli1:EGFP–cdc42wt)^{y48}* transgenic zebrafish, revealing similar vacuolar structures (arrows). **m**, **n**, Standard confocal imaging of doubly fluorescent ECs in *Tg(fli1:EGFP–cdc42wt)^{y48}* transgenic zebrafish injected with the *fli1:mRFP1-F* construct, showing that the EGFP–cdc42wt (**m**) and mRFP1-F (**n**) proteins colocalize to intracellular vacuolar structures. Scale bars, 10 μm (**a**–**g**), 1 μm (**h**), 25 μm (**i**, **k**), 15 μm (**j**, **l**).

[1]Laboratory of Molecular Genetics, and [2]Microscopy and Imaging Core, National Institute of Child Health and Human Development, National Institutes of Health, Bethesda, Maryland 20892, USA. [3]Department of Pathology, Texas A&M University System Health Science Center, 208 Reynolds Medical Building, College Station, Texas 77843-1114, USA.

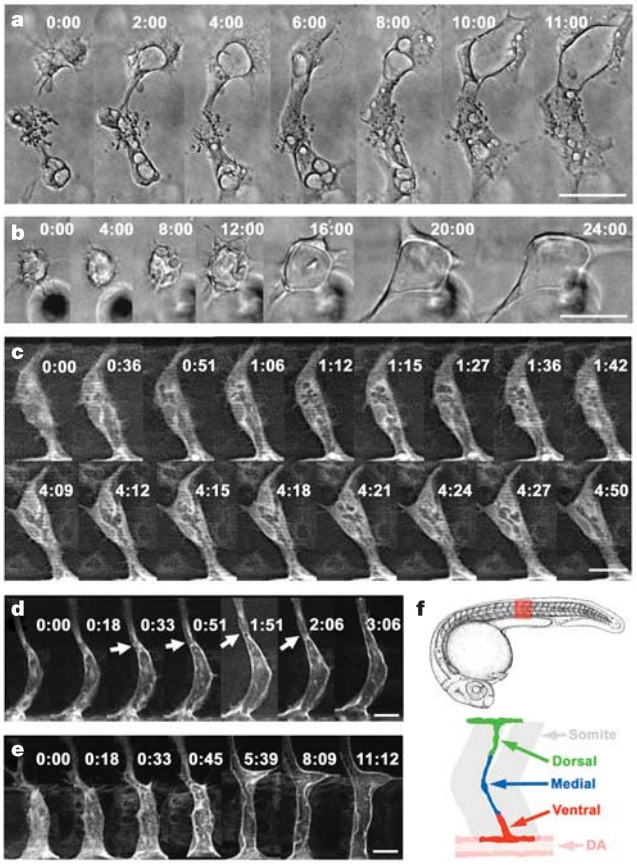

Figure 2 | Vacuoles are highly dynamic and fuse into large intracellular compartments. **a**, **b**, Time-lapse images of ECs in a 3D collagen gel, showing the formation of vacuoles and their fusion into larger intracellular compartments (**a**) and massive enlargement of the vacuolar compartment within a single EC (**b**). **c**–**e**, Two-photon time-lapse images of EGFP-positive ventral ECs in growing trunk intersegmental vessels in *Tg*(*fli1*:*EGFP–cdc42wt*)^{y48} transgenic animals, showing the emergence of vacuoles and their highly dynamic fusion into a larger intracellular compartments (**c**), and relatively rapid (**d**) or more prolonged (**e**) formation of enlarged lumenal spaces. Arrows in **d** indicate cell boundaries. **f**, Zebrafish intersegmental vessels are initially assembled from three cells arranged in a chain. The red box on the top drawing corresponds to the area depicted in the diagram below. Only the ventralmost intersegmental EC is imaged in **c**–**e**. See ref. 18 for additional information on zebrafish trunk vessel formation. DA, dorsal aorta. For each time-lapse sequence the time from the first frame of each successive image is shown in the format hours:minutes. Scale bars, 50 μm (**a**, **b**), 20 μm (**c**–**e**). See Supplementary Movies 1–5 for complete time-lapse sequences corresponding to **a**–**e**, respectively.

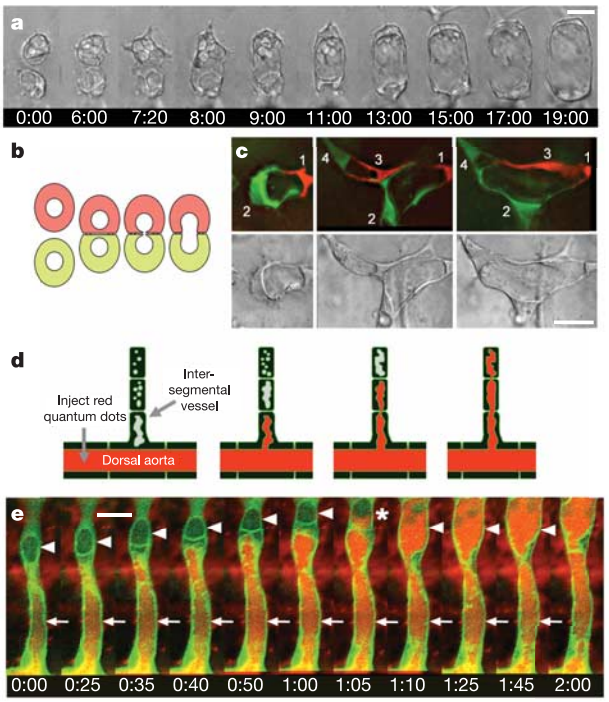

Figure 3 | Intracellular vacuolar compartments fuse to form intercellular lumenal spaces. **a**, Time-lapse images of two EC cells in a 3D collagen-gel matrix showing fusion of their intracellular vacuoles to generate a single large lumenal space. **b**, **c**, Fusion of intracellular vacuolar compartments preserves membrane topology and is not accompanied by cytoplasmic mixing. **b**, Differentially labelled ECs form junctions at points of cell–cell contact. Exocytosis of intercellular vacuoles into the cell–cell interface leads to formation of a common space bounded by both cells but sealed from the rest of the extracellular environment. **c**, Epifluorescence and light microscopy time-lapse images (top and bottom rows, respectively) of four HUVEC expressing either *EGFP–cdc42* (green) or *mRFP1-F* (red) in a 3D collagen gel. The red and green fluorophores do not mix after intercellular vacuole fusion. **d**, **e**, Intercellular transfer of vacuolar contents in intersegmental vessels undergoing tubular morphogenesis *in vivo*. **d**, Red quantum dots injected into the circulation are transferred from the lumenized dorsal aorta into preformed vacuolar compartments within proximal intersegmental ECs and are subsequently transferred serially to more distal intersegmental ECs. **e**, Two-photon time-lapse imaging of trunk intersegmental vessel sprouts in living *Tg*(*fli1*:*EGFP–cdc42wt*)^{y48} transgenic animals injected intravascularly with 605-nm quantum dots. Quantum dots are transferred from the dorsal aorta to vacuoles in proximal (arrows) and then more distal (arrowheads) intersegmental ECs. In frame 1:05 the vacuole in the distal EC was captured in the process of filling with quantum dots from the proximal cell below (asterisk). For each time-lapse sequence the time from the first frame of each successive image is shown in the format hours:minutes. Scale bars, 25 μm (**a**, **c**), 20 μm (**e**). Supplementary Movies 7–10 show complete time-lapse sequences corresponding to **a**, **c** and **e**.

defects in vascular development in *Tg*(*fli1*:*EGFP–cdc42wt*)^{y48} embryos and larvae; vessels displayed normal kinetics of appearance, anatomy and morphology[17,18], as well as normal vessel pathfinding behaviour[19] (data not shown).

We used two-photon imaging of the *Tg*(*fli1*:*EGFP–cdc42wt*)^{y48} line and/or confocal imaging of animals injected with the *fli1:mRFP1-F* construct to examine the formation and subsequent dynamics of vacuoles *in vivo*. We focused our initial efforts on the easily imaged, simple, and metamerically repeating system of angiogenic trunk intersegmental vessels[17]. Previous studies have shown that each intersegmental vessel is initially formed from three ECs that emerge from the dorsal aorta and migrate as a chain along myotomal boundaries[18–20]. Two-photon imaging of growing intersegmental vessels in living *Tg*(*fli1*:*EGFP–cdc42wt*)^{y48} embryos (Fig. 1k, l) revealed vacuolar structures similar to those observed in cultured human ECs during tube morphogenesis *in vitro* (Fig. 1i, j). Analogous subcellular structures were observed in confocal images of red fluorescent ECs in wild-type animals injected with a *fli1:mRFP1-F* construct, indicating that the vacuolar structures we observed were not an artefact of EGFP–cdc42wt expression (data not shown). Colocalization of perivacuolar red and green fluorescence in ECs of *Tg*(*fli1*:*EGFP–cdc42wt*)^{y48} embryos injected with *fli1:mRFP1-F* showed that both fluorescent probes highlight the same subcellular structures (Fig. 1m, n). Endothelial vacuoles were also readily observed in transmission electron micrographs of newly formed blood vessels in wild-type (non-transgenic) zebrafish embryos, with an appearance similar to that of vacuoles in electron micrographs of ECs developing lumens in 3D collagen gels (Fig. 1g, h). Together, these results show that vacuoles are present in ECs *in vivo* and can be imaged in live animals with fluorescent probes that highlight these structures in ECs *in vitro*.

We used time-lapse imaging to examine the dynamics of endothelial vacuoles and their contribution to vascular lumen formation. Time-

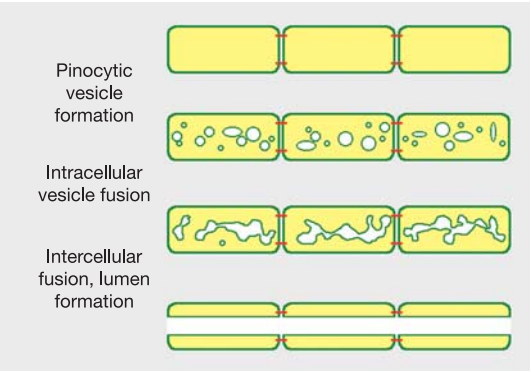

Figure 4 | A model for vascular lumen formation by intracellular and intercellular fusion of endothelial vacuoles. The diagram shows the mechanistic sequence of steps proposed to lead to intercellular lumen formation: intracellular vesicle formation, intracellular vesicle fusion, and finally intercellular merging of vacuolar compartments and lumen formation. These steps may not occur synchronously in all of the ECs in a lumenizing vessel but instead sequentially, as shown in Fig. 3d.

lapse imaging of cultured ECs reveals that endothelial vacuoles *in vitro* are highly dynamic, rapidly appearing and disappearing, fusing together and enlarging to create the lumenal space (Fig. 2a, and Supplementary Movie 1). Over time the vacuoles enlarge and coalesce to form nascent lumenal compartments encompassing most of the volume of the cell (Fig. 2b, and Supplementary Movie 2). High-resolution time-lapse two-photon imaging of lumenizing intersegmental vessels in *Tg*(*fli1*:*EGFP–cdc42wt*)^{y48} embryos with the use of a novel continuous-flow imaging chamber[21] and a sensitive direct detector array revealed very similar vacuolar dynamics *in vivo* (Fig. 2c–e, and Supplementary Movies 3–6; vessels imaged in Fig. 2c–e are shown schematically in Fig. 2f). Vacuoles appear, disappear and fuse to form larger compartments on a timescale of minutes (Fig. 2c, and Supplementary Movie 3). At later stages, vacuoles merge into nascent lumenal compartments filling most of the cell, as in ECs *in vitro* (Fig. 2d, e, and Supplementary Movies 4–6 provide examples of the range of behaviours observed in lumenizing vessels). These nascent lumenal compartments remain extremely dynamic, with membrane protrusions continuously extending and retracting into the lumenal space. Standard confocal imaging of red fluorescent ECs in wild-type embryos injected with the *fli1:mRFP1-F* construct revealed similar vacuolar dynamics (data not shown), indicating that our observations do not reflect abnormal consequences of EGFP–cdc42wt fusion protein expression.

We next investigated whether the enlarged vacuolar compartments that we observed within different ECs *in vitro* and *in vivo* underwent fusion to generate multicellular lumenal spaces. Time-lapse microscopy of ECs in 3D collagen gels revealed ECs forming extensive cell–cell contacts followed by a merging of their intracellular vacuolar compartments (Fig. 3a, and Supplementary Movie 7). For a further examination of the nature of these fusion events *in vitro* we differentially labelled the cytoplasm of cultured ECs to determine whether intercellular vacuole fusion was accompanied by cytoplasmic fusion (Fig. 3b, c). We found that in all cases vacuole fusion occurred without cytoplasmic mixing (Fig. 3c, and Supplementary Movies 8 and 9), indicating that the formation of a common lumenal space might occur by the exocytosis of intracellular vacuoles into junctional spaces between adjacent ECs (Fig. 3b). We performed additional experiments to determine whether fusion of preformed vacuolar compartments of separate ECs occurs *in vivo* and whether this is relevant to lumenization. We injected red quantum dots intravascularly to label the circulation of *Tg*(*fli1*:*EGFP–cdc42wt*)^{y48} embryos, and then examined whether the quantum dots were later transferred from the patent dorsal aorta to unlabelled vacuolar/nascent lumenal compartments of ECs of the adjacent developing intersegmental vessels (Fig. 3d, e). Serial transfer of the red fluorescent label could be observed from the dorsal aorta into previously unlabelled vacuolar compartments of the proximal intersegmental EC and then more distal ECs (Fig. 3e, and Supplementary Movie 10). These results indicate that preformed vacuolar compartments in adjacent ECs become linked to form a continuous lumenal space in developing blood vessels *in vivo*.

Together, our results *in vitro* and *in vivo* support a proposed model in which the formation and intracellular and intercellular fusion of endothelial vacuoles drives vascular lumen formation (Fig. 4). Recent studies in both *Drosophila* and *Caenorhabditis elegans* indicate that intracellular lumen formation might be a common general mechanism for tube formation during development[22–25]. We find no evidence for endothelial apoptosis during early vascular development, precluding models for vascular cavitation (death of the central cells in an endothelial cord to create a hollow space; V. Pham, personal communication). Although we have not yet performed a similar careful time-lapse analysis of larger-calibre blood vessels, lumen formation within larger aggregates or cords of ECs may occur through cord hollowing[1]. This process would be mechanistically analogous to what we have observed for the intersegmental vessels—exocytosis of vacuoles into a common intercellular space bounded by multiple ECs (instead of just two cells) that are joined together by junctional contacts would lead to the formation of a common lumenal space sealed off from the rest of the extracellular environment. It remains to be seen to what extent the molecular machinery involved in vascular lumen formation resembles that employed for other vacuolar/vesicular trafficking processes, such as vesicle trafficking at neuronal synapses[26,27] or transvascular exchange and vascular permeability across endothelial monolayers[28,29].

METHODS

Zebrafish husbandry and generation of transgenic lines. Zebrafish husbandry and maintenance were performed as described[30]. Molecular cloning and construction of vectors used for transgenesis in this study were conducted with standard methods. Transient and germline transgenic zebrafish lines used in this study were generated with methods described previously[16]. Additional details are given in Supplementary Methods.

Endothelial cell culture and 3D collagen vasculogenesis assays. Human umbilical vein EC culture and 3D collagen vasculogenesis assays were performed as described[10]. Additional details on cell culture and vectors and methods used for transfection and viral infection are given in Supplementary Methods.

Microscopy and imaging. Time-lapse imaging of zebrafish embryos was conducted as described[14,21]. Intravascular injection of quantum dots was performed as described[14]. Additional details are given in Supplementary Methods. Time-lapse imaging of cultured human umbilical vein ECs was conducted with a temperature-controlled imaging chamber at 37 °C with a continuous flow of 5% CO_2. Images were captured with a Nikon Eclipse TE2000-U inverted microscope. Additional details are given in Supplementary Methods.

Received 19 January; accepted 19 May 2006.
Published online 21 June 2006.

1. Lubarsky, B. & Krasnow, M. A. Tube morphogenesis: making and shaping biological tubes. *Cell* **112,** 19–28 (2003).
2. Downs, K. M. Florence Sabin and the mechanism of blood vessel lumenization during vasculogenesis. *Microcirculation* **10,** 5–25 (2003).
3. Folkman, J. & Haudenschild, C. Angiogenesis by capillary endothelial cells in culture. *Trans. Ophthalmol. Soc. U. K.* **100,** 346–353 (1980).
4. Folkman, J. & Haudenschild, C. Angiogenesis *in vitro*. *Nature* **288,** 551–556 (1980).
5. Bayless, K. J. & Davis, G. E. The Cdc42 and Rac1 GTPases are required for capillary lumen formation in three-dimensional extracellular matrices. *J. Cell Sci.* **115,** 1123–1136 (2002).
6. Bayless, K. J., Salazar, R. & Davis, G. E. RGD-dependent vacuolation and lumen formation observed during endothelial cell morphogenesis in three-dimensional fibrin matrices involves the $\alpha_v\beta_3$ and $\alpha_5\beta_1$ integrins. *Am. J. Pathol.* **156,** 1673–1683 (2000).
7. Davis, G. E. & Bayless, K. J. An integrin and Rho GTPase-dependent pinocytic vacuole mechanism controls capillary lumen formation in collagen and fibrin matrices. *Microcirculation* **10,** 27–44 (2003).
8. Davis, G. E., Bayless, K. J. & Mavila, A. Molecular basis of endothelial cell

morphogenesis in three-dimensional extracellular matrices. *Anat. Rec.* **268,** 252–275 (2002).
9. Davis, G. E., Black, S. M. & Bayless, K. J. Capillary morphogenesis during human endothelial cell invasion of three-dimensional collagen matrices. *In Vitro Cell. Dev. Biol. Anim.* **36,** 513–519 (2000).
10. Davis, G. E. & Camarillo, C. W. An $\alpha_2\beta_1$ integrin-dependent pinocytic mechanism involving intracellular vacuole formation and coalescence regulates capillary lumen and tube formation in three-dimensional collagen matrix. *Exp. Cell Res.* **224,** 39–51 (1996).
11. Johnson, D. I. Cdc42: An essential Rho-type GTPase controlling eukaryotic cell polarity. *Microbiol. Mol. Biol. Rev.* **63,** 54–105 (1999).
12. Hancock, J. F., Cadwallader, K. & Marshall, C. J. Methylation and proteolysis are essential for efficient membrane binding of prenylated p21K-ras(B). *EMBO J.* **10,** 641–646 (1991).
13. Campbell, R. E. *et al.* A monomeric red fluorescent protein. *Proc. Natl Acad. Sci. USA* **99,** 7877–7882 (2002).
14. Kamei, M., Isogai, S. & Weinstein, B. M. Imaging blood vessels in the zebrafish. *Methods Cell Biol.* **76,** 51–74 (2004).
15. Weinstein, B. Vascular cell biology *in vivo*: a new piscine paradigm? *Trends Cell Biol.* **12,** 439–445 (2002).
16. Lawson, N. D. & Weinstein, B. M. *In vivo* imaging of embryonic vascular development using transgenic zebrafish. *Dev. Biol.* **248,** 307–318 (2002).
17. Isogai, S., Horiguchi, M. & Weinstein, B. M. The vascular anatomy of the developing zebrafish: an atlas of embryonic and early larval development. *Dev. Biol.* **230,** 278–301 (2001).
18. Isogai, S., Lawson, N. D., Torrealday, S., Horiguchi, M. & Weinstein, B. M. Angiogenic network formation in the developing vertebrate trunk. *Development* **130,** 5281–5290 (2003).
19. Torres-Vazquez, J. *et al.* Semaphorin-plexin signaling guides patterning of the developing vasculature. *Dev. Cell* **7,** 117–123 (2004).
20. Childs, S., Chen, J. N., Garrity, D. M. & Fishman, M. C. Patterning of angiogenesis in the zebrafish embryo. *Development* **129,** 973–982 (2002).
21. Kamei, M. & Weinstein, B. M. Long-term time-lapse fluorescence imaging of developing zebrafish. *Zebrafish* **2,** 113–123 (2005).
22. Berry, K. L., Bulow, H. E., Hall, D. H. & Hobert, O. A. *C. elegans* CLIC-like protein required for intracellular tube formation and maintenance. *Science* **302,** 2134–2137 (2003).
23. Buechner, M. Tubes and the single *C. elegans* excretory cell. *Trends Cell Biol.* **12,** 479–484 (2002).
24. Manning, G. & Krasnow, M. in *The Development of* Drosophila melanogaster (eds Martinez-Arias, A. & Bate, M.) 609–685 (Cold Spring Harbor Laboratory Press, Cold Spring Harbor, New York, 1993).
25. Paul, S. M. & Beitel, G. J. Developmental biology. Tubulogenesis CLICs into place. *Science* **302,** 2077–2078 (2003).
26. Rizzoli, S. O. & Betz, W. J. Synaptic vesicle pools. *Nature Rev. Neurosci.* **6,** 57–69 (2005).
27. Sudhof, T. C. The synaptic vesicle cycle. *Annu. Rev. Neurosci.* **27,** 509–547 (2004).
28. Carver, L. A. & Schnitzer, J. E. Caveolae: mining little caves for new cancer targets. *Nature Rev. Cancer* **3,** 571–581 (2003).
29. Schnitzer, J. E. Caveolae: from basic trafficking mechanisms to targeting transcytosis for tissue-specific drug and gene delivery *in vivo*. *Adv. Drug Deliv. Rev.* **49,** 265–280 (2001).
30. Westerfield, M. *The Zebrafish Book* (Univ. Oregon Press, Eugene, Oregon, 1995).

Supplementary Information is linked to the online version of the paper at www.nature.com/nature.

Acknowledgements We thank J. Faske for technical assistance, G. Martin for help in constructing the mRFP1-expressing human ECs, K. Tanegashima for assistance with western blot analysis, R. Tsien for providing the mRFP1 vector, and I. B. Dawid for critical reading of this manuscript. This work was supported in part by a grant from the NIH to G.E.D. B.M.W. is supported by the intramural program of the NICHD.

Author Information Reprints and permissions information is available at npg.nature.com/reprintsandpermissions. The authors declare no competing financial interests. Correspondence and requests for materials should be addressed to B.M.W. (bw96w@nih.gov).